GLOBAL EFFECTS OF SOFTENING n-BODY GALAXIES

RICHARD A. GERBER
Space Science Division, NASA Ames Research Center, M.S. 245-3, Moffet Field, CA 94035

ABSTRACT

Softening of the gravitational potential in n-body simulations, introduced as a modification to Newtonian gravity on the small scale, can affect the large-scale, global dynamics of computer models of galaxies. These effects arise because softening modifies the gravitational binding energy and changes the equilibrium configuration of self-gravitating systems.

In this paper we give the analytic expressions for the "softened" gravitational potential energy of some example systems. We then present a corrected form of the scalar virial theorem, which describes the relationship between potential and kinetic energies in equilibrium galaxies.

It is important to understand these phenomena when conducting numerical experiments on galaxies. It is often desired to numerically construct and study an equilibrium galaxy derived from an analytic model. We show by example that the use of softening can lead to global phenomena that cannot be discussed solely in terms of Newtonian gravity. As an example, we examine numerically the behavior of a spherical galaxy undergoing fundamental mode oscillations as the softening length is varied.

Subject headings: galaxies: kinematics and dynamics — galaxies: structure — methods: numerical

1. INTRODUCTION

Because large-scale changes in galaxies occur on time-scales measured in units of 10^8 yr, n-body computer models provide the only way to perform dynamical experiments on these systems. But even with today's most powerful supercomputers, it is not feasible to calculate the trajectories of all 10^{11} stars that constitute a typical large galaxy. Therefore, the numerical experimenter must make compromises when modeling the relevant physics with a computer.

A common practice is to represent a galaxy with fewer "particles" than the number of stars that are present in a real galaxy. The number of particles, n, must be chosen large enough to reduce "n-body noise" (i.e., artificially imposed graininess in the gravitational potential calculation) and suppress unwanted two-body gravitational scattering. In a real galaxy, like the Milky Way, there are so many stars and the space between individual stars is so immense that relaxation effects due to two-body scattering are insignificant over a Hubble time. In order to ensure the collisionless nature of the system, the gravitational potential is "softened" in numerical simulations. Softening, first introduced by Aarseth (1963), has the effect of reducing two-body short-range forces.

A common strategy in astrophysical n-body experiments is to replace the $1/r$ point mass potential by one of the Plummer form:

$$\Phi(r) = -\frac{GM}{\sqrt{r^2 + a^2}}, \qquad (1)$$

where a denotes the "softening length" and M is the mass of the "particle." This expression does not have the infinity at $r = 0$ that is present in the point mass potential; instead the force on a test particle goes to zero at zero separation (see eq. [3] below). Softening has the additional beneficial effect of allowing a larger time step to be taken in the simulation (see, e.g., Hockney & Eastwood 1988).

Softening also has its drawbacks since it compromises the physics that the experimenter desires to model. As Dyer & Ip (1993) pointed out, the standard scheme is physically inconsistent. The Plummer potential is that which would be produced by a density distribution of

$$\rho(r) = \frac{3M}{4\pi a^3} \left(1 + \frac{r^2}{a^2}\right)^{-5/2}. \qquad (2)$$

However, when forces are calculated between particles the expression used is

$$F(r) = -\frac{GM^2 r}{(r^2 + a^2)^{3/2}}, \qquad (3)$$

which is correct only for a point mass interacting with a Plummer density distribution. Dyer & Ip (1993) compare (1) the generally used form, (2) the true force between two Plummer spheres, and (3) that between two (unsoftened) point masses. The three expressions converge at approximately $r = 5a$, but at smaller separations they differ significantly (see Dyer & Ip 1993). In typical three-dimensional self-gravitating n-body experiments, galaxies with diameters on the order of 25–100 resolution, or softening, lengths are used.

Of the three forms considered by Dyer & Ip, the standard Plummer-point mass interaction produces the smallest (in magnitude) maximum force. In this paper we refer to particles that interact in the manner given by equation (3) as "Plummer point masses," which describes well their dual extended/point character.

It is generally recognized that softening strongly affects an n-body simulation over length scales comparable to the softening length. For example, it has long been known that softening modifies the dispersion relation in stellar disks and therefore influences the local stability of those disks (see e.g., Miller 1972; Toomre 1977; and recently Romeo 1994). Sellwood (1981) notes that excessive softening can suppress the bar instability in disks.

The purpose of this paper to is point out that global, or "long-wavelength," phenomena are also influenced when a softened form of the gravitational potential is employed in numerical experiments. We seek to determine under which situations the method provides a faithful representation of the desired physics.

For example, the total gravitational potential energy of a softened n-body system is always less (in absolute magnitude) than in the Newtonian case. The large-scale force field is also changed. These modifications can have important dynamical effects that must be understood when building model galaxies and analyzing results from computational experiments. Softening affects many familiar results from Newtonian gravitational physics, including the familiar form of the scalar virial theorem, which relates time averages of kinetic and potential energies.

In § 2 we show how softening changes the calculation of forces and gravitational potential energies, and we give the relevant form of the virial theorem. In § 3 we show by example how softening can affect the global behavior of an n-body galaxy.

2. EFFECTS OF SOFTENING

In this section we examine how the presence of softening affects some of the standard results of Newtonian gravitational physics. First we look at Newton's First Theorem, which concerns the force felt by a particle inside a spherical shell of matter. The modified form of some force laws for some example spherical three-dimensional mass distributions are discussed, and then we present the modified form of the virial theorem for a configuration composed of Plummer point masses.

2.1. Newton's First Theoreem

The well-known result that a test particle placed within a thin spherical shell of matter feels no net force is referred to as Newton's First Theorem (Binney & Tremaine 1987). When mass elements on the spherical shell behave like Plummer point particles, however, the Theorem is no longer true.

2.1.1. A Heuristic Argument

Before we derive an exact expression for the gravitational potential due to a spherical shell of Plummer point masses, we make an intuitive argument that the dynamics needs to be changed. To do this, we follow a modified form of the discussion given in Binney & Tremaine (1987).

Consider a particle of mass M placed at point P somewhere inside a constant density spherical shell of radius R as shown in Figure 1. A diameter is shown passing through P and the center of the shell, C. A line is drawn passing through P, and it is rotated around the diameter passing through P and C. This produces two cones as shown in the figure. Assume the solid opening angle of these cones is small so that $r_1 + r_2 \approx 2R$. The cones intersect amounts of mass on the shell we denote δM_1 and δM_2.

Consider the force felt by P due to δM_1 and δM_2, which are composed of Plummer point masses. The result is

$$F_1 = \frac{GM \, \delta M_1 r_1}{r_1^2 + a^2} = \frac{GM \, \delta M_1}{r_1^2}\left(1 + \frac{a^2}{r_1^2}\right)^{-3/2}, \quad (4)$$

$$F_2 = -\frac{GM \, \delta M_2 r_2}{r_2^2 + a^2} + \frac{GM \, \delta M_2}{r_2^2}\left(1 + \frac{a^2}{r_2^2}\right)^{-3/2}. \quad (5)$$

Geometrical considerations alone give the result that

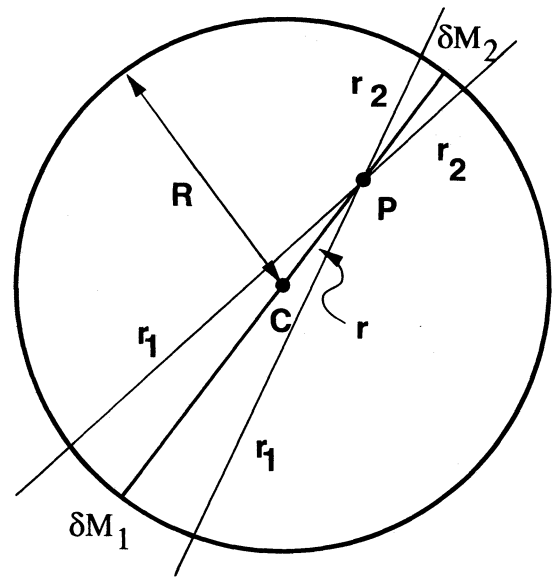$$\frac{\delta M_1}{r_1^2} = \frac{\delta M_2}{r_2^2}. \quad (6)$$

We also note the relationships (see Fig. 1) $r_1 = R + r$ and $r_2 = r - R$, and we can write the net radial force on P as

$$F_{net} = F_1 - F_2 = \frac{GM \, \delta M_2}{R^2(1 + r/R)^2}$$

$$\left\{\left[1 + \frac{a^2}{R^2(1 - r/R)^2}\right]^{-3/2} - \left[1 + \frac{a^2}{R^2(1 + r/R)^2}\right]^{-3/2}\right\}. \quad (7)$$

Inside the shell $r \leq R$, and the first term in braces is always smaller than the second, which gives a radially inward net force. This is easily understood in the limit that the test particle lies very close to δM_1. Then the force due to δM_1 tends toward zero and the net force is entirely produced by δM_2. In the Newtonian case the two mass elements always exert equal and opposite forces on M and the net force is zero. Note that by setting $a = 0$ we recover the Newtonian result (i.e., $F_{net} = 0$) in equation (7).

2.1.2. An Exact Expression for the Potential

We now derive an exact expression for the gravitational potential due to a spherical shell of material that interacts gravitationally like Plummer point masses. The author would like to thank R. H. Miller for much of the derivation in this section.

First consider the standard Newtonian integral form of the Poisson equation,

$$\Phi(x) = G\int \frac{\rho(x')}{|x - x'|}\,d^3x'. \quad (8)$$

If we let x lie along the z-axis, we have in spherical coordinates,

$$\Phi(r, \theta, \phi) = G\int \frac{\rho(r', \theta', \phi')}{\sqrt{r^2 + r'^2 - 2rr'\cos\theta'}}$$

$$r'^2\,dr'\cos\theta'\,d\theta'\,d\phi'. \quad (9)$$

A standard way to solve the integral is to expand the denominator in terms of powers of the radius and spherical harmonics (see, e.g., Jackson 1975),

$$\Phi(r, \theta, \phi) = 4\pi G \sum_{l,m} \frac{1}{2l + 1}$$

$$\times \left[\int \frac{r_-^l}{r_+^{l+1}} Y_{lm}^*(\theta', \phi') \rho(r', \theta', \phi') r'^2 \, dr' \sin \theta' \, d\theta' \, d\phi' \right]$$

$$Y_{lm}(\theta, \phi) , \quad (10)$$

where r_- (r_+) is the lesser (greater) of r and r'. With softening included, equation (9) becomes

$$\Phi(r, \theta, \phi) = G \int \frac{\rho(r', \theta', \phi')}{\sqrt{r^2 + r'^2 + a^2 - 2rr' \cos \theta'}}$$

$$\times r'^2 \, dr' \cos \theta' \, d\theta' \, d\phi' . \quad (11)$$

If we can write the denominator in the form $(\xi^2 + \eta^2 - 2\xi\eta \cos \theta)^{1/2}$ for the same θ as in equation (10) then we can use the same series expansion to solve the problem. The requirement that the two expressions for the denominator be equal makes $\xi\eta = rr'$ and $\xi^2 + \eta^2 = r^2 + r'^2 + a^2$. These equations are solved with

$$2\xi = \sqrt{(r + r')^2 + a^2} + \sqrt{(r - r')^2 + a^2} , \quad (12)$$

$$2\eta = \sqrt{(r + r')^2 + a^2} - \sqrt{(r - r') + a^2} . \quad (13)$$

The potential is then

$$\Phi(r, \theta, \phi) = 4\pi G \sum_{l,m} \frac{1}{2l + 1}$$

$$\times \left[\int \frac{\eta^l}{\xi^{l+1}} Y_{lm}^*(\theta', \phi') \rho(r', \theta', \phi') r'^2 \, dr' \sin \theta' \, d\theta' \, d\phi' \right]$$

$$Y_{lm}(\theta, \phi) . \quad (14)$$

For a spherical shell of mass M with radius R, the density is

$$\rho(r', \theta', \phi') = \frac{M}{R^2} \delta(R - r') Y_{00}(\theta', \phi') \quad (15)$$

and by the orthogonality of the spherical harmonics, equation (14) is

$$\Phi(\xi) = -\frac{GM}{\xi} . \quad (16)$$

It is convenient to rewrite ξ by introducing two dimensionless "lengths," α and β,

$$\xi = \frac{a}{2} \left[\sqrt{(\alpha + \beta)^2 + 1} + \sqrt{(\alpha - \beta)^2 + 1} \right] , \quad (17)$$

where

$$\alpha = \frac{R}{a} , \quad \beta = \frac{r}{a} \quad \text{for } r > R ,$$

$$\alpha = \frac{r}{a} , \quad \beta = \frac{R}{a} \quad \text{for } r < R .$$

In Figure 2 we plot the acceleration as a function of radius for the shell. Inside the shell there is always an inward force that reaches zero only at the center. Outside the shell the magnitude of the force is less than the Newtonian result.
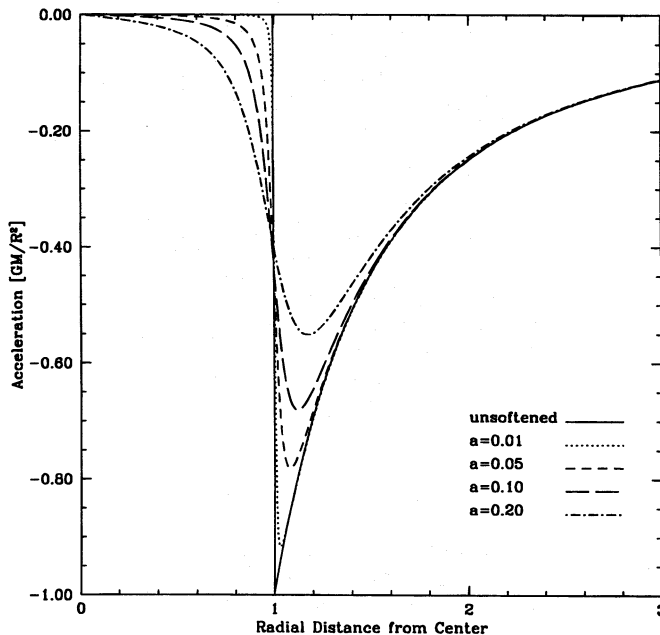

FIG. 2.—The acceleration produced by a constant density spherical shell for different values of the softening length. The shell has a radius of 1. Values are scaled so that the acceleration just outside the shell has the value 1 in the unsoftened case.

Near the center of the shell we can obtain an estimate of the character of the force field by expanding the potential in powers of r/a and find

$$\Phi = \frac{-GM}{a\sqrt{\beta^2 + 1}} + \frac{1}{2} \frac{GM}{a(\beta^2 + 1)^{5/2}} \alpha^2 + O(\alpha^3) . \quad (18)$$

The first term is a constant and does not contribute to the force. The second term represents a harmonic term: a test mass will oscillate about the center of the shell with angular frequency, ω,

$$\omega^2 = \frac{GM}{a^3(\beta^2 + 1)^{5/2}} = \frac{GMa^2}{(R^2 + a^2)^{5/2}} . \quad (19)$$

For a given mass the frequency goes to zero as $1/\beta^{5/2} = (a/R)^{5/2}$.

2.2. Global Forces

The force produced by a spherical three-dimensional configuration can be found by summing spherical shells. In general, softened force fields appear to differ from unsoftened ones in regions when the radial density gradient is large compared with the softening length.

As n-body representations of galaxies must always be finite, we examine two truncated spherical mass distributions as example cases: (1) a constant density sphere and (2) a singular isothermal sphere.

The potential inside any spherical Plummer point particle distribution with outer radius R can be written as

$$\Phi(r, R, a) = -4\pi G a^3 \left[\int_0^{r/a} \frac{\rho(\alpha)\alpha^2 \, d\alpha}{\xi} + \int_{r/a}^{R/a} \frac{\rho(\beta)\beta^2 \, d\beta}{\xi} \right] , \quad (20)$$

where ξ was defined previously in equation (17).

2.2.1. Constant Density Sphere

Analytic expressions for the potential and force due to a truncated constant density sphere are given in the Appendix. The fractional deviation from the unsoftened force is plotted in Figure 3 for a constant density sphere of radius $R = 1$ and softening lengths of 0.01, 0.05, 0.1, and 0.2. Two effects are of note: (1) The largest deviations from the unsoftened force occur near the outer edge and (2) with a truncated radius of 100 or more softening lengths (i.e., 200 softening lengths across the configuration) the error is less than 2% everywhere.

An unsoftened uniform density sphere produces a radial force that increases linearly with radius, i.e., it has a harmonic oscillator potential which has an angular frequency

$$\omega_{\text{true}}^2 = \frac{4}{3}\pi G\rho . \tag{21}$$

By expanding the softened potential in powers of r/a about the origin, we find that the lowest order term in the force represents an oscillator with frequency

$$\omega_{\text{soft}}^2 = \omega_{\text{true}}^2 \left[\frac{\chi^3}{(1 + \chi^2)^{3/2}}\right], \tag{22}$$

where $\chi \equiv (R/a)$. The softened frequency approaches the true frequency very quickly as the softening length gets smaller than the actual size of the configuration. Even with R as small as $10a$, ω is modified by a multiplicative factor of only 0.9926. Note that this result was obtained for radii less than the softening length, implying that, at least in this case, softening by itself has essentially no effect on the dynamics of a test particle orbiting very near the center.

2.2.2. Isothermal Sphere

In Figure 4 we plot the circular speed of a truncated singular isothermal sphere of radius $R = 1$ where the unsoftened circular speed has been normalized to 1. A

Fig. 4.—The circular speed ("rotation curve") for an isothermal sphere density distribution, which has been truncated at a radius $R = 1$. Units are normalized so that the unsoftened isothermal sphere has a circular speed of 1.

closed-form expression for the force is given in the Appendix.

With softened gravity, the circular speed is zero at the origin and remains about 2% below the unsoftened case at 10 softening lengths away from the center. With a system radius of 100 softening lengths, the circular speed is within 1% of the Newtonian value over 90% of the configuration. However, with relatively small softening lengths such as $R/a = 10$, the rotation curve is not flat and does not much resemble a true isothermal sphere.

2.3. The Virial Theorem

The familiar form of the scalar virial theorem states that, in equilibrium, a self-gravitating system obeys

$$\langle T \rangle = -\frac{1}{2}\langle U \rangle ,$$

where $\langle T \rangle$ and $\langle U \rangle$ are time averages of the total kinetic and total potential energy, respectively. With softened gravity, this relationship is modified.

Elementary mechanics texts (see e.g., Marion 1970) give a more general form of the virial theorem,

$$\langle T \rangle = -\frac{1}{2}\left\langle \sum_\alpha \mathbf{r}_\alpha \cdot \mathbf{F}_\alpha \right\rangle , \tag{23}$$

where the sum is over all particles and $\mathbf{F}$ is the force on particle α. If the force can be written as the gradient of a potential energy function, U, we can write

$$\langle T \rangle = -\frac{1}{2}\left\langle \sum_\alpha \mathbf{r}_\alpha \cdot \nabla U_\alpha \right\rangle . \tag{24}$$

For the Plummer point masses we have

$$\mathbf{r}_\alpha \cdot \nabla U_\alpha = -\frac{GM^2 r_\alpha^2}{(r_\alpha^2 + a^2)^{3/2}} = \left(\frac{r_\alpha^2}{r_\alpha^2 + a^2}\right)U_\alpha , \tag{25}$$
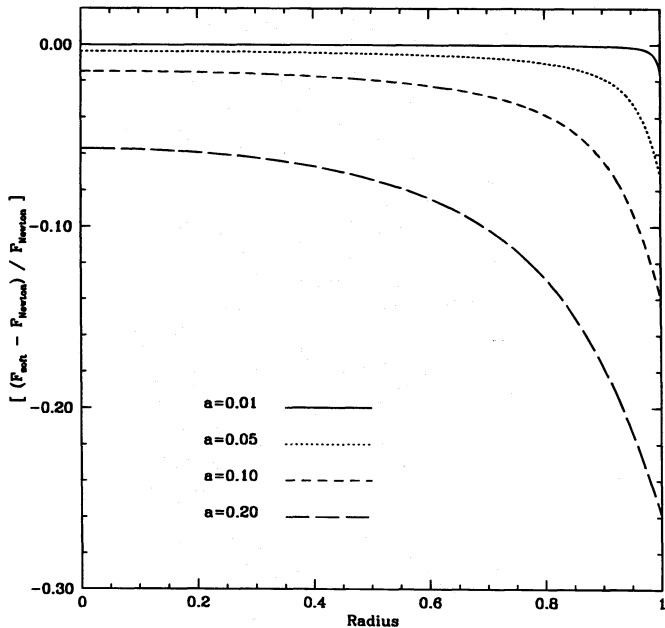

Fig. 3.—The fractional difference between the softened force the unsoftened force for a constant density sphere, which has been truncated at a radius $R = 1$. The fractional deviation is calculated as $(F_{\text{softened}} - F_{\text{unsoftened}})/F_{\text{unsoftened}}$.
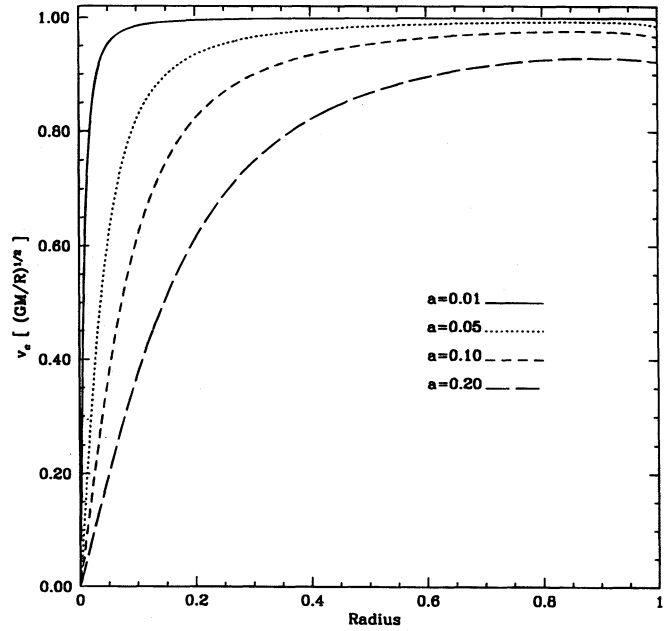
and the virial theorem becomes

$$\langle T \rangle = -\frac{1}{2} \left\langle \sum_\alpha \left(\frac{r_\alpha^2}{r_\alpha^2 + a^2} \right) U_\alpha \right\rangle . \quad (26)$$

With $a = 0$, we have the standard Newtonian result. Note that here U is not the Newtonian potential energy, but rather the potential energy due to point-mass interactions with Plummer spheres. Even taking that into consideration, the familiar virial theorem is modified by the extra factor involving the softening length.

For a continuous spherical system of radius R and total mass M we can write

$$\langle T \rangle = -\pi \int_0^R \frac{r'^4 \rho(r', R, M) \Phi(r', R, M, a) dr'}{r'^2 + a^2} , \quad (27)$$

or, by defining $\eta \equiv r'/a$ and $\chi \equiv R/a$,

$$\langle T \rangle = -\pi a^3 \int_0^\chi \frac{\eta^4 \rho(\eta, \chi, R, M) \Phi(\eta, \chi, R, M) d\eta}{\eta^2 + 1} . \quad (28)$$

If we write the density and potential in the following form, absorbing geometrical factors into new functions, Γ and Φ,

$$\rho(\eta, \chi, M, R) = \frac{M}{R^3} \Gamma(\eta, \chi) \quad (29)$$

and

$$\Phi(\eta, \chi, M, R) = \frac{GM}{R} \phi(\eta, \chi) , \quad (30)$$

we obtain

$$\langle T \rangle = -\frac{\pi GM^2}{R\chi^3} \int_0^\chi \frac{\Gamma(\eta, \chi) \phi(\eta, \chi) \eta^4 \, d\eta}{\eta^2 + 1} . \quad (31)$$

The integral in equation (31) is just now a dimensionless number, depending on the value of χ, i.e., the size of the system in terms of the softening length. The integral can be evaluated numerically for various density distributions and values of χ.

As an example, we show in Figure 5 the softened virial relationship for the conical model of radius R that will be discussed further in the next section. (The potential for the softened conical model is given in the Appendix.) This plot (analogous ones can be derived for any given density distribution) shows how Plummer softening influences the equilibrium configuration of a self-gravitating system. With no softening, $-\langle U \rangle = 2\langle T \rangle$ at the numerical value indicated by the horizontal line in Figure 5. With softening included, the identical density distribution is in equilibrium with a value of $-\langle U \rangle$ less than the softened case and a numerical value of $2\langle T \rangle$ that is lower still.

As in the previous discussion, the virial relationship is close to that for the unsoftened case for $R/a \gtrsim 100$. The horizontal line shows the familiar Newtonian value at which $-\langle U \rangle = 2\langle T \rangle$. For softening lengths that are large compared to the system size, there is a significant change from the Newtonian case. At $a/R = 0.1$ the virial theorem relationship is modified at approximately the 10% level. This corresponds to a model galaxy with a diameter of $20a$.

2.4. A Word about n-Body Codes

The previous discussion was based solely on analytic, continuous models of softened gravity. In n-body simula-
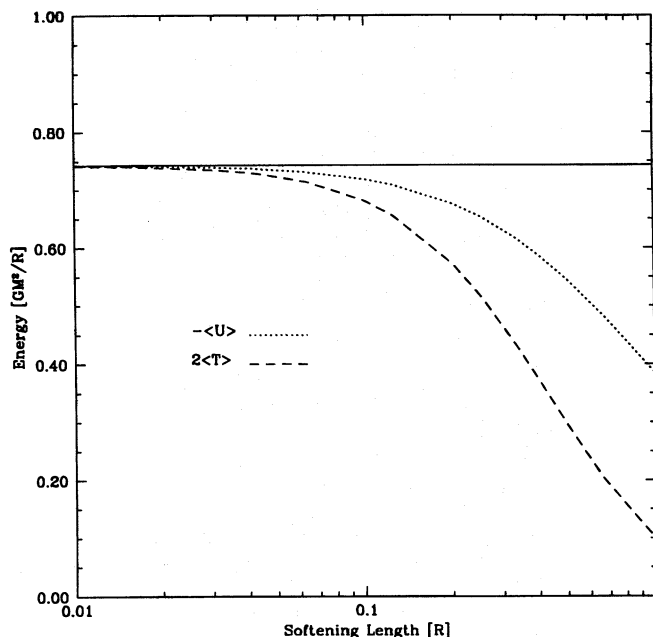

FIG. 5.—The equilibrium values of (negative) the (softened) potential energy and twice the total kinetic energy as given by the "softened" virial theorem for the conical model. The softening length is given in units of the radius of the conical model. In the absence of softening, both lines would lie on the horizontal line shown in the plot.

tions gravitational force calculations are further influenced by finite particle number and numerical methods. Two popular methods for calculating the gravitational potential in galaxy simulations are Particle Mesh (PM) and tree codes, which both employ softened gravity, but not in the same manner.

In tree codes, the softened force between nearby particles is calculated directly. Particles are grouped into a "tree" hierarchy, and the potential due to distant groups of particles is approximated by a multipole moment expansion, usually truncated at either the monopole or quadrupole term. This distant field approximation is not accounted for by the discussion of the previous sections.

In PM codes, each particle's mass is assigned in some manner to a regular grid (mesh) during the calculation of the gravitational potential. Softening is applied to the mesh.

In practice, these further approximations will give any given code an effective softening length that is not necessarily equal to the value of a that is explicitly entered into the simulation.

In § 3 we show by example how softening can affect the behavior of an n-body galaxy, and we use the results of this section to find a numerical representation of a spherical galaxy that is approximately in a "softened" virial equilibrium.

3. AN EXAMPLE OF THE GLOBAL EFFECTS OF SOFTENING

A stable spherical galaxy, if perturbed, has been shown to undergo undamped global oscillations (Miller & Smith 1994). We have confirmed Miller & Smith's basic result that their conical model supports large fundamental mode oscillations that are undamped over at least 80 dynamical time-scales. These oscillations were observed using both a tree code obtained from L. Hernquist and two different PM

momentum-conserving codes written by the author of this paper. The oscillations in the global kinetic energy of one such model are shown in Figure 6. The oscillations in kinetic energy have been shown to be a good diagnostic of the fundamental mode oscillations described by Miller & Smith (1994) and show the remarkable undamped nature of the oscillations. Runs were started from a 10,240 particle load provided by R. Miller. To test the effect of particle number, some test runs were performed with 122,880 particles and the main points discussed below were unaffected. Phase space parameters for the load were produced by sampling from a distribution function that describes the conical model of total mass M and radius R. The density, ρ, is given by $\rho = \rho_c(1 - r/R)$ if $0 < R/r < 1$ and $\rho = 0$ otherwise; $\rho_c = 3M/(\pi R^3)$.

The conical model's ability to sustain these modes gives us a tool with which to explore the effect of softening on a global property of a spherical galaxy. We will show that the exact same initial state (i.e., identical initial phase space coordinates) oscillates in a quantitatively different manner depending on the choice of the softening length. We will use the amplitude of the approximately sinusoidal oscillations in total kinetic energy to describe the behavior of the system.

Starting with a particle load that was derived using strictly Newtonian gravity, we follow that load's evolution using softening gravity. Because the initial particle velocities were assigned based on an unsoftened analytic model, the configuration does not have the instantaneous value of total kinetic energy, T, equal to the time-averaged value, $\langle T \rangle$, appropriate for a finite value of the softening length. This provides an initial perturbation that gets the system oscillating. The galaxy oscillates about the equilibrium state

appropriate for the given values of the softening length. That state cannot be precisely predicted for this initial load since the density distribution changes once the configuration is released from its initial state. However, if the "softened" equilibrium is not too "far" from the original one, then the amplitude, T_0, of the kinetic energy oscillation can be approximated by

$$T_0 \approx |\, T_{\text{initial}} - \langle T_{\text{soft,analytic}} \rangle \,|, \qquad (32)$$

where $\langle T_{\text{soft,analytic}} \rangle$ is given by equation (31). This expression states that, since the oscillations are undamped, the amplitude should be equal to the difference between the initial kinetic energy and equilibrium value of the kinetic energy.

In Figure 7 we show the time dependence of the total kinetic energy for three different values of the softening length using a PM code. It can be seen that the amplitude increases with increasing softening length. This is due to the galaxy, in its initial state, being "farther away" from the "softened" equilibrium state. The oscillation frequency also depends on the softening length. This is no surprise since the frequency is a function of the gravitational potential energy (see Miller & Smith 1994).

Figure 8 shows the rms amplitude of kinetic energy oscillations for different values of softening using the tree code and the PM code. Also shown is the crude estimate of the expected amplitude based on equation (32). In Figure 9 we show the corresponding values of $\langle T \rangle$. These values of softening are in a "typical" range for n-body simulations, i.e., $R/a \approx 20$–100.

A number of features are of note in Figures 8 and 9. First is that they quantitatively show that the oscillation amplitude increases and $\langle T \rangle$ decreases with increasing softening. Note that in Figure 8 a minimum in the amplitude occurs at the point with the value of $a/R = 0.02226$. This occurs
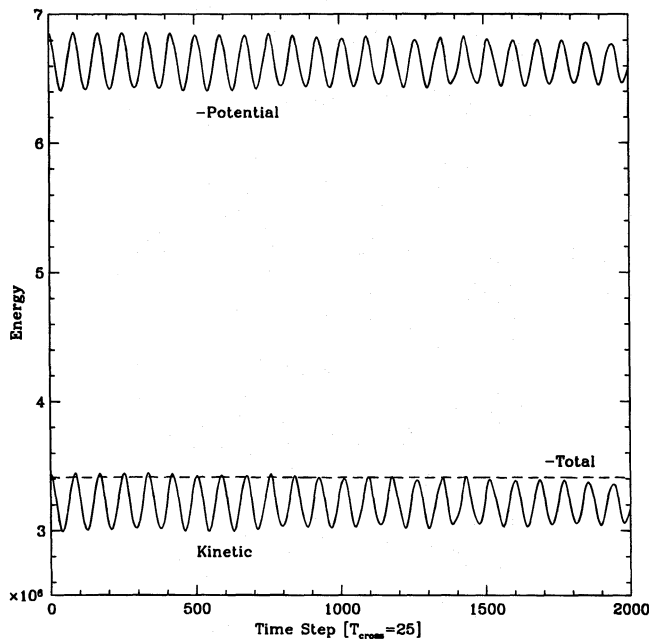

FIG. 6.—Values of total kinetic, potential, and total energy for the conical model ($R = 11.23$, $a = 0.5$). The sinusoidal time variations continue essentially undamped for 80 crossing times. These are the same oscillations reported by Miller & Smith (1994). The results presented here were obtained using a particle-mesh n-body code that was developed independently from that used by Miller & Smith. Similar results were obtained using a tree code, as discussed in the text.
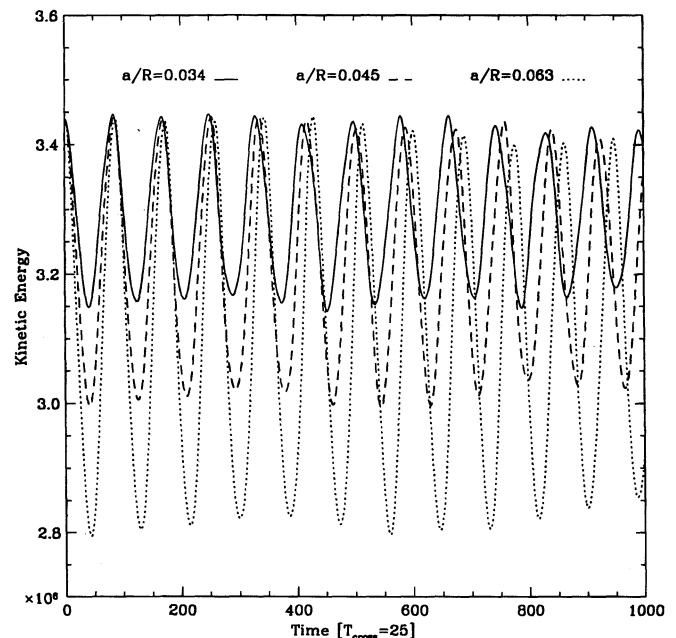

FIG. 7.—Variations in kinetic energy as the conical model is evolved using three different values of the softening length. In all cases a 64^3 particle-mesh code was employed. The three values of a correspond to $a/R = 0.031, 0.045, 0.063$. $n = 10,240$.
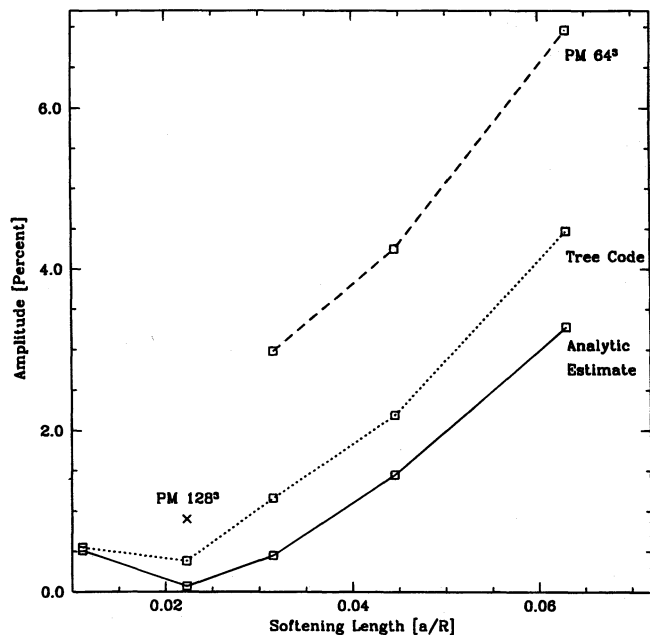
FIG. 8.—The amplitude of kinetic energy oscillations, given as a percentage of the total kinetic energy, for the conical model of radius R. The PM 64^3 runs were performed using a 64^3 grid spacing, $\Delta L/R = 0.089$. The PM 128^3 run used $\Delta L/R = 0.0445$. For comparison the estimate given in the text is shown. The experimental amplitudes are rms values.

because the kinetic energy in the initial particle load was not set precisely to its unsoftened analytic value (as derived from a distribution function) and, by coincidence, this one model's initial kinetic energy was closest (one part in 10^{-3}) to the value of $\langle T \rangle$ predicted by the softened virial theorem (as given by equation [31]). This means that this model was
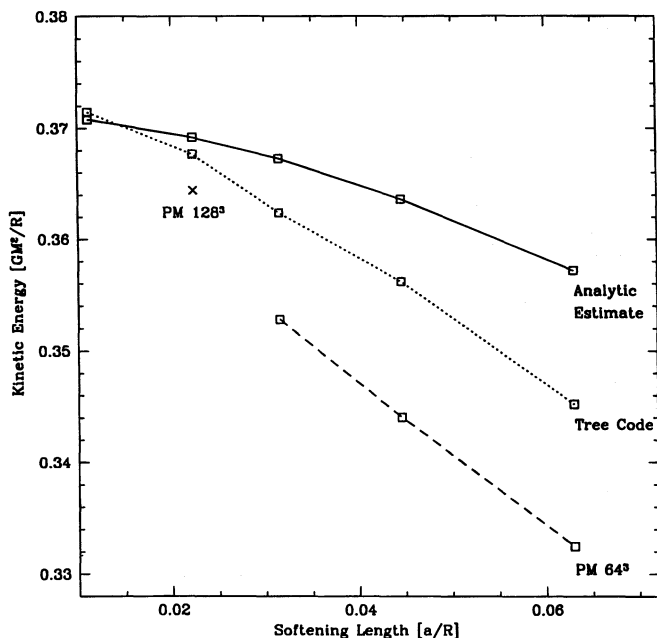

FIG. 9.—The total kinetic energy averaged over many cycles of the oscillations for the same computer runs as given in the previous figure. The estimate is based on the "softened" virial theorem as discussed in the text.

initially "closest" to its "softened" equilibrium state and therefore oscillated with the smallest amplitude.

The plots reveal that the PM code has a larger "effective softening" than the tree code for a given value of a. This is due to the manner in which mass is assigned to the grid and how force values are interpolated from the grid to the particle positions.

Note that we have not determined nor discussed the character of the oscillations themselves beyond reproducing the computational results given by Miller & Smith (1994). Those results, that the global oscillations persist undamped over timescale approaching a Hubble time, have been verified here, and further investigation into the nature of the oscillations will be the subject of another paper (Gerber, Miller, & Smith 1996).

For those interested in further details of the runs, some are given here. For the tree code, the accuracy parameter was $\theta = 0.75$, and quadrupole terms were included. For the PM code, the CIC scheme was used (see Hockney & Eastwood 1988), with 64^3 or 128^3 grid points and a grid spacing of $\Delta L = 0.089R$ ($2a$). The specific computational values for the conical model were: $G = 1$, $M = 10240$, $R = 11.23$.

4. SUMMARY

We have shown that softening of the gravitational potential, introduced as a modification to Newtonian gravity on the small scale, can have an effect on the global behavior of n-body computer models of galaxies. Global force fields, values of the potential energy, and the familiar form of the virial theorem are all modified by the use of softened gravity. Expressions have been given to calculate these quantities and relationships.

It is important to understand the phenomena discussed in this paper when conducting numerical experiments on galaxies. It is often desirable to construct an "equilibrium" galaxy with phase space parameters derived from an analytic model, and then perturb the galaxy to study its time evolution. As shown in this paper, the use of softening can lead to global, or "long-wavelength," behavior that cannot be discussed solely in terms of Newtonian gravity.

The role of softening also should be considered in attempts to use multiple softening lengths within a single simulation (to try to resolve dense regions, for example). Multigrid and nested grid numerical schemes may also be affected, particularly if the system reaches or passes through an equilibrium or quasi-equilibrium state. Any abrupt change in the softening length (either spatially or temporally) will force the system out of equilibrium without changing any of the true physical parameters of the system.

APPENDIX

Here we give the expressions for the softened potential for ($r < R$) of the constant density sphere of radius R, the softened force for the singular isothermal sphere truncated at radius R, and the softened potential for the conical model.

For a constant density sphere of total mass M,

$$\Phi = -\frac{3GM}{4\chi^2 R}\left[3\eta \ln(C+\eta) + 3\eta\ln(C-\eta) - \eta^2 B + 2\chi^2 B + \eta\chi B + 2B + \eta\chi A\right.$$

$$\left. -3\eta\ln(A+\chi-\eta) - 3\eta\ln(B+\chi+\eta) + \eta^2 A - 2\chi^2 A - 2A\right],$$

where

$$\eta \equiv \frac{r}{a}, \qquad \chi \equiv \frac{R}{a}, \qquad A \equiv \sqrt{\eta^2+\chi^2-2\eta\chi+1}, \qquad B \equiv \sqrt{\eta^2+\chi^2+2\eta\chi+1}, \qquad C \equiv \sqrt{\eta^2+1}.$$

For a truncated isothermal sphere of radius R and total mass M,

$$F_r = \frac{-GM}{2aR\eta^2\sqrt{\eta^2+1}}\left[-\sinh^{-1}\left(\frac{\eta\chi+\eta^2+1}{\chi}\right) + BC - AC - \sinh^{-1}\left(\frac{\eta\chi-\eta^2-1}{\chi}\right)\right].$$

The potential for the conical model is

$$\Phi = \frac{MG}{4\chi^3\eta R}\left[-4\eta^3 C + 26\eta C - 3\ln(C-\eta) + 3\ln(C+\eta) + 3\ln(A+\chi-\eta)\right.$$

$$-5B\chi - 13\eta B + 2\eta^2\chi B + 5A\chi + 2\eta^3 B + 2\eta^3 A - 13\eta A - 3\ln(B+\chi+\eta) - 2\eta A\chi^2$$

$$-12\eta^2\ln(A+\chi-\eta) + 12\eta^2\ln(B+\chi+\eta) + 12\eta^2\ln(C-\eta) - 12\eta^2\ln(C+\eta) - 12\chi\eta\ln(C-\eta)$$

$$\left. +12\chi\eta\ln(B+\chi+\eta) + 12\chi\eta\ln(A+\chi-\eta) - 12\chi\eta\ln(C+\eta) - 2B\chi^3 + 2A\chi^3 - 2\chi^2\eta B - 2\eta^2\chi A\right].$$

REFERENCES

Aarseth, S. 1963, MNRAS, 126, 223
Binney, J., & Tremaine, S. 1987, Galactic Dynamics (Princeton: Princeton Univ. Press)
Dyer, C. C., & Ip, P. S. S. 1993, ApJ, 60, 409
Gerber, R. A., Miller, R. H., & Smith, B. F. 1996, in preparation
Hockney, R. W., & Eastwood, J. W. 1988, Computer Simulations Using Particles (Bristol: Adam Hilger)
Jackson, J. D. 1975, Classical Electrodynamics (New York: Wiley)
Marion, J. B. 1970, Classical Dynamics of Particles and Systems (New York: Academic)
Miller, R. H. 1972, in Proc. IAU Colloq. 101, Gravitational n-body Problem ed. M. Lecar (Dordrecht: Reidel), 213
Miller, R. H., & Smith, B. F. 1994, Celes. Mech. Dyn. Astron., 59, 161
Romeo, A. B. 1994, A&A, 286, 799
Sellwood, J. A. 1981, A&A, 99, 362
Toomre, A. 1977, ARA&A, 15, 437